

1
2
3
4
5
6
7
8
9

Supplementary Information for

Ammonia emission abatement does not fully control reduced
forms of nitrogen deposition

Jiani Tan, Joshua S. Fu, John H. Seinfeld
Correspondence to: jsfu@utk.edu or seinfeld@caltech.edu

Materials and Methods

Site measurement of deposition and air concentrations. Site observations of wet NO_3^- deposition and wet NH_4^+ deposition were provided by the National Trends Network (NTN) of the National Atmospheric Deposition Program (NADP) (<http://nadp.slh.wisc.edu/NTN/>). NTN measured the precipitation chemistry, including precipitation amount and concentrations of free acidity H^+ , conductance, calcium, magnesium, sodium, potassium, sulfate, NO_3^- , NH_4^+ and chloride, at 373 sites located throughout the entire U.S. (Fig. S4) from 1980s until present day. The sites were located away from urban and point pollution sources. Samples were collected weekly in wet deposition collectors and shipped in bottles to the Illinois State Water Survey at the University of Illinois at Urbana-Champaign (before March 1, 2018) and the Central Analytical Laboratory at the Wisconsin State Laboratory of Hygiene (after March 1, 2018). The data quality has been evaluated with the NTN procedures and documentation (<http://nadp.slh.wisc.edu/lib/qaReports.aspx>). This study used the annual accumulated wet deposition data from 244 sites with available data in the study period (Table S2). Site observations of airborne NO_2 concentrations were provided by Air Quality System (AQS) Monitoring Network of U.S. EPA (<https://www.epa.gov/air-trends/nitrogen-dioxide-trends>). AQS observed the airborne concentrations of CO_2 , PM, NO_2 , O_3 and SO_2 at 153 sites over U.S. (Fig. S5 and Table S2).

The Ammonia Monitoring Network (AMoN) of NADP (<http://nadp.slh.wisc.edu/AMoN/>) provides airborne NH_3 concentrations beginning in 2007. The raw dataset can be downloaded from the AMoN website at <http://nadp.slh.wisc.edu/AMoN/>. According to Table S1, the number of measurement sites increased considerably after 2011. Thus, we use only the data after 2011 in this study. We plotted the NH_3 air concentration with N deposition, NO_2 air concentrations and N emissions (same data as Fig. 1 in the main manuscript) in Figure S1. Note that the base year for calculating the percentage changes is 2011 (in Fig. S1) instead of 2002 (in Fig. 1), because fewer measurements for NH_3 air concentration exist before 2011.

Annual gradient maps of deposition. Spatial distributions of NO_y and NH_x deposition were developed by the Total Deposition Science Committee (TDEP) of NADP by spatial interpolation of quality-controlled observation sites with model simulations (<http://nadp.slh.wisc.edu/NTN/maps.aspx>). Maps were available from 1985 to 2017. The quality and uncertainty associated with these maps have not been fully evaluated, an uncertainty that may affect the interpretation of the results.

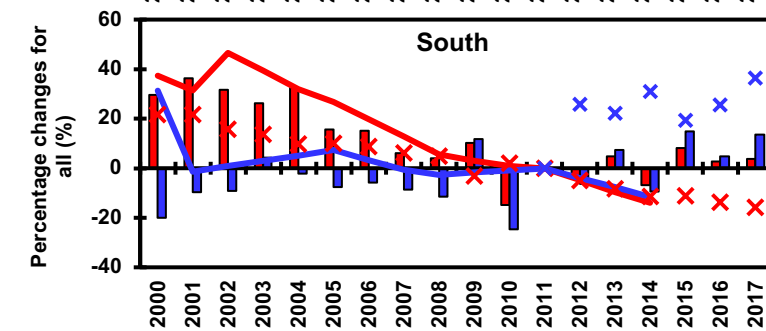
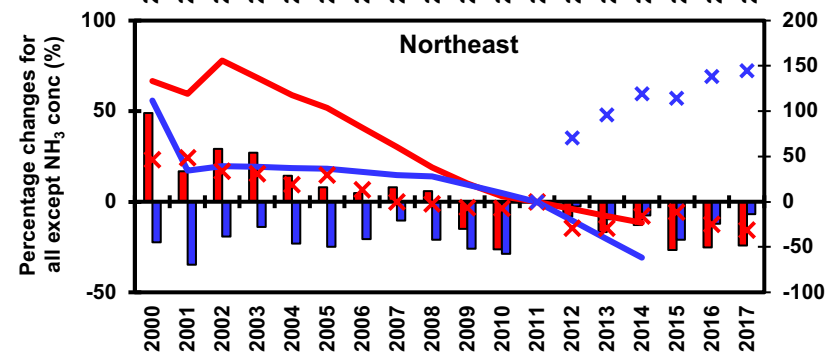
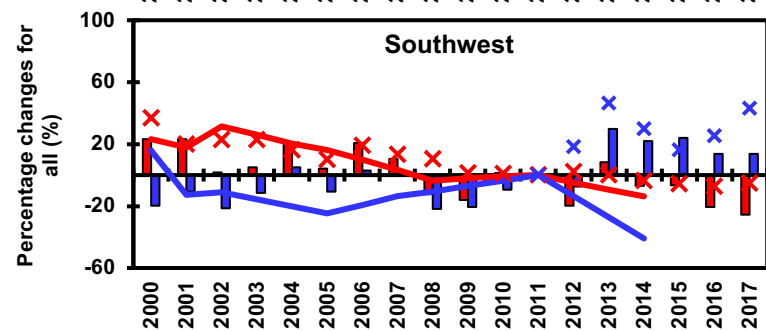
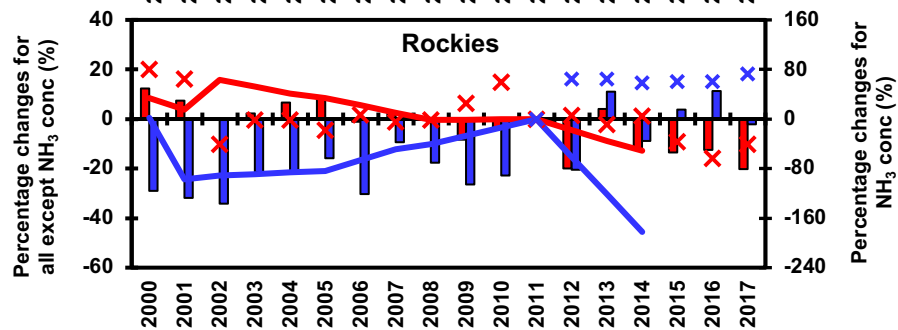
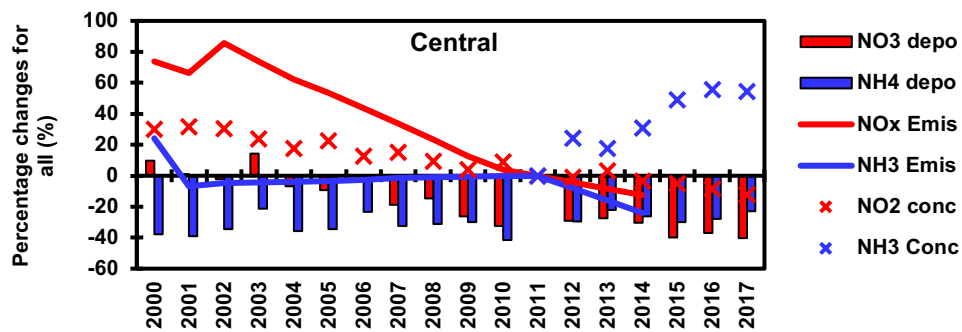
Emissions. NO_x and NH_3 emissions were provided by U.S. EPA's National Emissions Inventory (NEI) (<https://www.epa.gov/air-emissions-inventories/national-emissions-inventory-nei>). Annual emissions at the country scale were available during 2000-2014. Annual emissions of individual states were available only for years 2002, 2005, 2008, 2011 and 2014. Contiguous emissions for other years were calculated by linear interpolation of country-scale data. We compared this emission dataset with site observations of wet deposition and air concentration. Comparability was subject to the extent to which the NADP sites are more or less evenly located. In this regard, stations in western and central U.S. tended to be more scattered than those in the eastern U.S. (Figs. S4-S5 and Table S2). Further analysis with more observation data is suggested for these regions. Spatial distributions of emissions were obtained from the Emissions Database for Global Atmospheric Research (EDGARv4.3.2) (<http://edgar.jrc.ec.europa.eu/overview.php?v=432>). Spatial resolutions of both NO_x and NH_3

emissions were 0.1×0.1 degree ($\sim 11.1 \text{ km} \times 11.1 \text{ km}$). The EDGAR emissions over CONUS were developed based on information from U.S. EPA NEI (S1).

Modeling. The response of deposition to emission control was determined from simulated NO_y and NH_x deposition from multi-model mean (MMM) results of eleven global climate models from the Task Force on Hemispheric Transport of Air Pollution (HTAP) second phase, directed by the United Nations Economic Commission for Europe (UNECE) (<http://www.htap.org/>) (S2). The participating models were CAM-Chem, CHASER_rel, CHASER_t106, EMEP_rv48, GEMMACH, GEOS5, GEOSSCHEMAJOINT, OsloCTM3v.2, GOCARTv5, SPRINTARS, and C-IFS_v2. Spatial resolutions of the models ranged from $0.5^\circ \times 0.5^\circ$ to $2.8^\circ \times 2.8^\circ$. All models used the anthropogenic emission inventory of HTAP v2.2 (S3), which is a harmonized emission inventory with inputs from U.S. EPA, Environment Canada, the European Monitoring and Evaluation Programme (EMEP), the Netherlands Organisation for Applied Scientific Research (TNO), the Model Intercomparison Study for Asia (MICS-Asia III), and the Emission Database for Global Atmospheric Research (EDGAR v4.3). All model predictions were interpolated to a uniform $0.1^\circ \times 0.1^\circ$ resolution to form the MMM results by linear interpolation. Simulations were conducted for 2010, with an additional six months as spin-up. Model mass balances were confirmed by comparison of outputs (depositions) with inputs (emissions) (S4).

MMM performance on wet deposition of NO_y and NH_x was evaluated with the U.S. NADP observation network (Reference S4 and Fig. S6). Predicted sum of gas-phase SO_2 wet deposition and aerosol SO_4^{2-} wet deposition was compared with observed SO_4^{2-} wet deposition (Fig. S6A,B). Predicted sum of gas-phase HNO_3 wet deposition and aerosol NO_3^- wet deposition was compared with observed NO_3^- wet deposition (Fig. S6C,D). NO_3^- wet deposition was overestimated by 20% with an R value of 0.9, with a general tendency of overestimation in the Midwest and Southeast. Predicted sum of gas-phase NH_3 wet deposition and aerosol NH_4^+ wet deposition was compared with observed NH_4^+ wet deposition (Fig. S6E,F). NH_4^+ wet deposition at most sites was well simulated with $R = 0.9$ and a slope of 0.8, with underestimation found in the Southeast. Simulation of dry deposition is subject to considerable uncertainty (S4), owing to lack of comprehensive observation data (S4, S5).

Emission Control Scenario. The base case utilized the HTAP v2.2 emissions inventory. In the emission control scenario, a modified emissions inventory was used with 20% reduction of all anthropogenic emissions, including SO_2 , NO_x , and NH_3 over North America. Since only anthropogenic emissions were reduced and natural emissions were not changed, the predicted percentage change of emissions, which included changes in both anthropogenic and natural emissions, was not equal to 20% (Fig. S3). Since the meteorological fields and model parameters remained unchanged in the base case and control scenarios, emissions change is the main factor contributing to the variation of deposition. The 20% reduction in anthropogenic emissions was considered as a reasonable perturbation to achieve a significant change, and at the same time an affordable target for an emissions reduction policy.



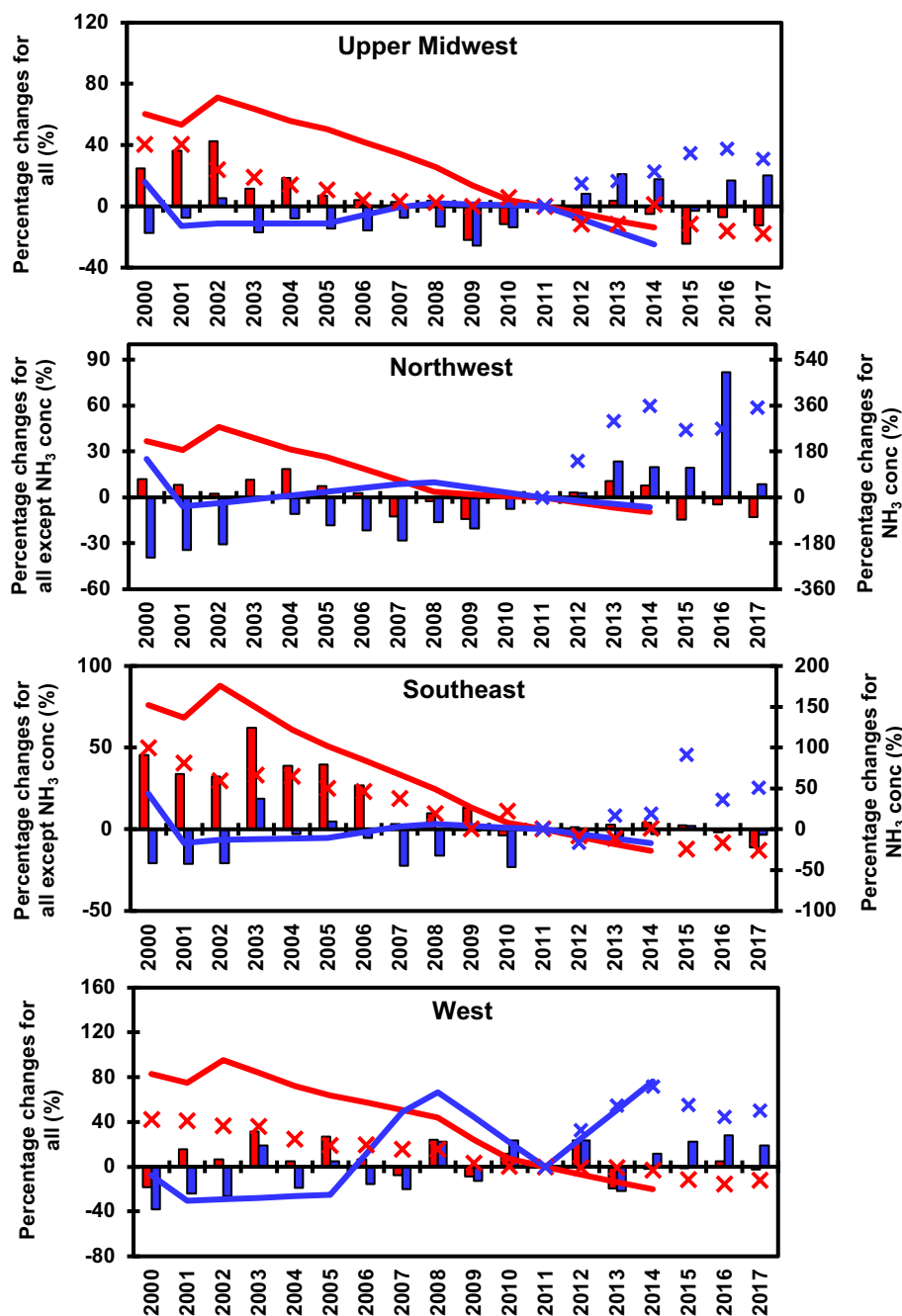


Figure S1. Percentage changes of N emissions, NO₂ and NH₃ air concentrations and N deposition in regions (%). The percentage changes were calculated based on 2011 level (i.e. $100 \times [\text{Emission of target year} - \text{Emission of 2011}] / [\text{Emission of 2011}]$).

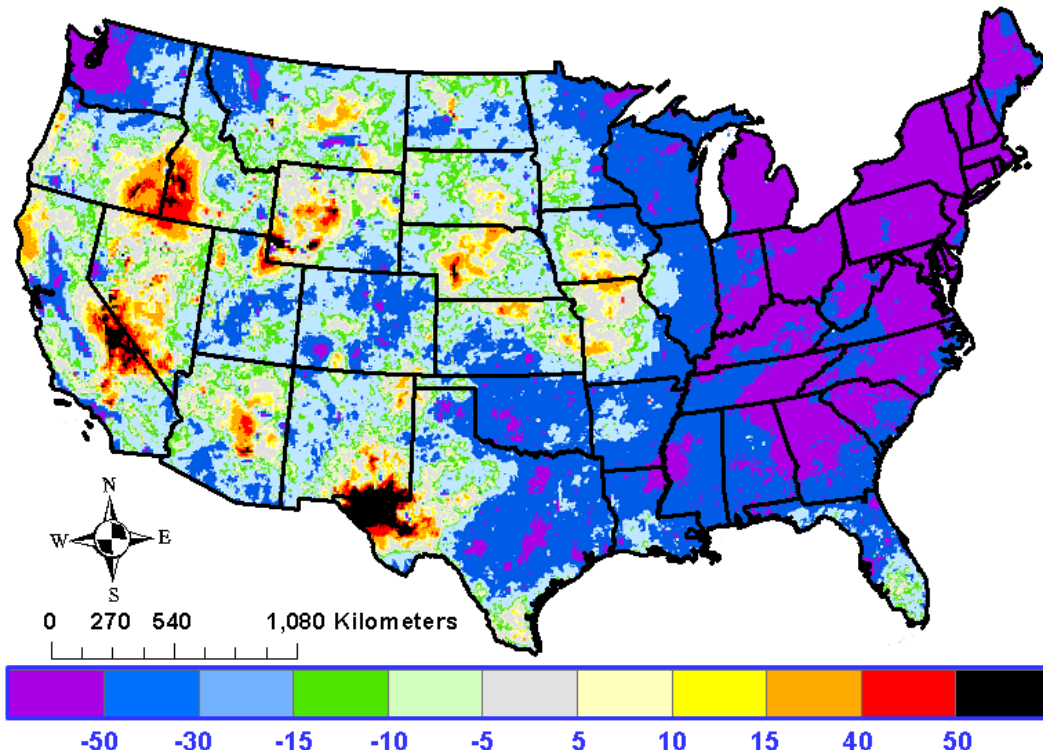


Fig. S2. Percentage change of S (wet + dry) deposition from 2001 to 2010 (calculated as $\frac{[2010] - [2001]}{[2001]} \times 100\%$) (unit: %). Spatial distributions of deposition were interpolation maps from NADP site observation (see Materials and Methods).

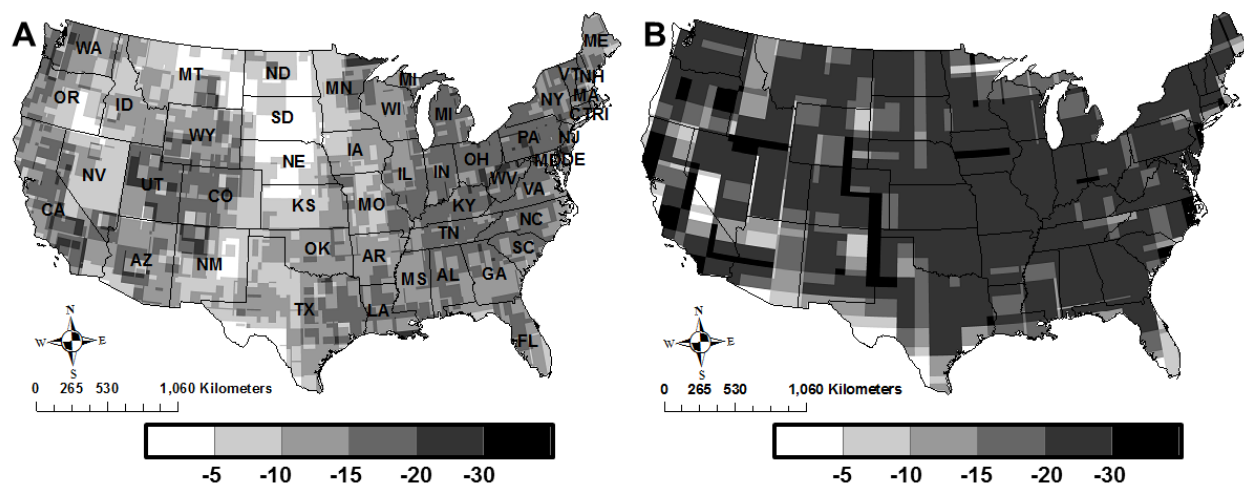


Fig. S3. Percentage changes of (A) NO_x emissions and (B) NH₃ emissions in the emission control scenarios (%).

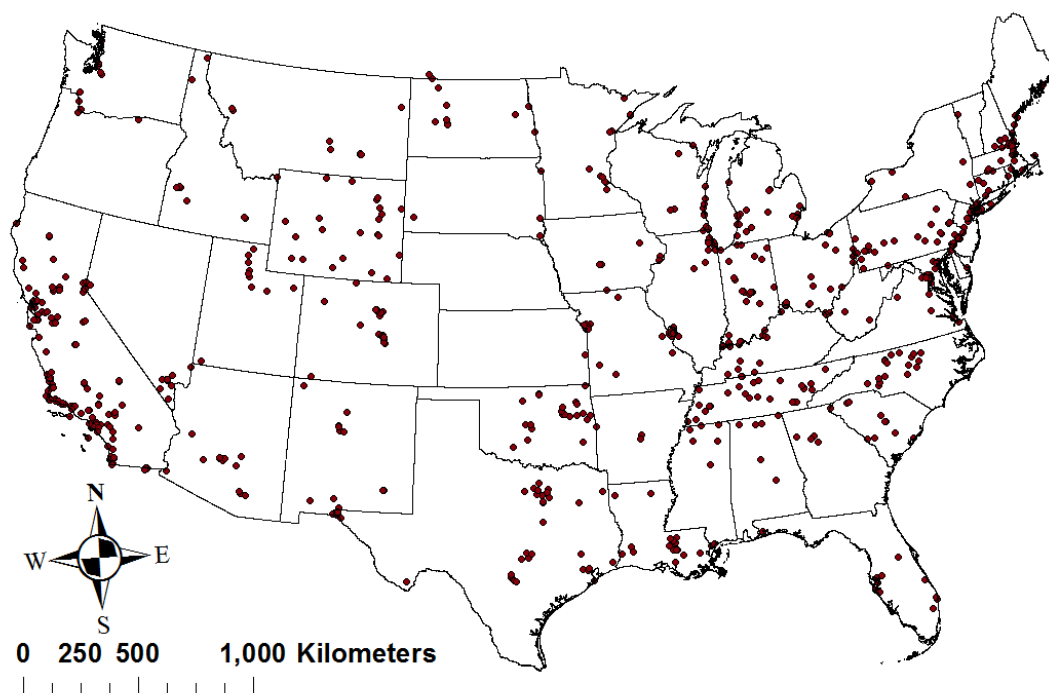


Fig. S5. Location of AQS sites for NO₂ air concentration over CONUS.

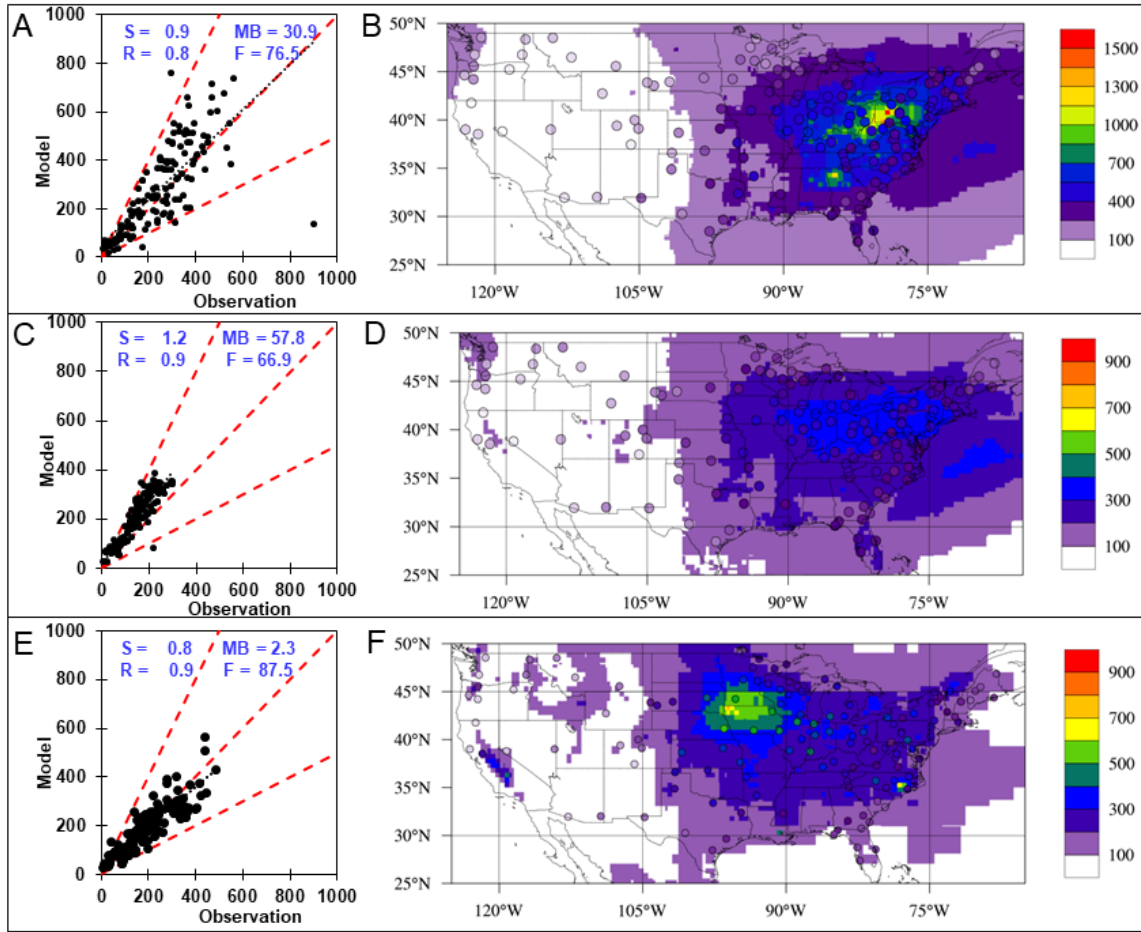


Fig. S6. Performance of HTAP-II multi-model mean (MMM) results on wet deposition over CONUS (unit: $\text{mg (N or S) m}^{-2} \text{ yr}^{-1}$). Adopted from Figure 1 and Figure 2 of Tan et al., 2018 (S4). (A-B) Evaluation on wet SO_4^{2-} deposition. (C-D) evaluation on wet NO_3^- deposition. (E-F) evaluation on wet NH_4^+ deposition. Contours are MMM results and filled circles are observations from NADP. MMM is the annual wet deposition in 2010 and the observation is 3-year average annual data of 2009-2011. Note for abbreviations: S-slope between observation and model results; MB-mean bias calculated as subtracting mean values of observations from mean values of model results; R-correlation coefficient; F-fraction of models results within $\pm 50\%$ of observations.

Table S1. Number of sites for NH₃ ambient concentrations in each region.

Regions	2007	2008	2009	2010	2011	2012	2013	2014	2015	2016	2017
Central	4	4	5	4	11	11	12	12	20	20	21
Northeast	1	1	3	5	8	13	13	15	20	24	24
Northwest	-	-	-	1	2	2	2	2	3	3	4
Rockies	-	-	-	-	2	3	3	3	5	6	6
South	3	3	3	3	6	5	5	5	11	11	11
Southeast	1	5	5	5	10	11	11	11	14	15	15
Southwest	1	3	3	3	8	9	9	10	10	10	10
Upper Midwest	5	5	5	3	4	4	4	4	8	8	8
West	-	-	-	-	3	3	3	3	3	3	3
Total	15	21	24	24	54	61	62	65	94	100	102

Table S2. Numbers of sites for NO₂ ambient concentrations and N wet deposition in each region from 2000 to 2017. Insufficient NO₂ observation exist in the Northwest.

Regions	AQS sites for NO ₂ ambient concentration	NADP sites for N wet deposition
Central	12	31
Northeast	25	36
Northwest	-	15
Rockies	6	22
South	36	25
Southeast	14	37
Southwest	10	31
Upper Midwest	2	32
West	48	15
Total	153	244

References

- S1. M. Crippa *et al.* Gridded emissions of air pollutants for the period 1970-2012 within EDGAR v4.3.2. *Earth Syst. Sci. Data* **10**, 1987-2013 (2018).
- S2. S. Galmarini *et al.* Technical note: Coordination and harmonization of the multi-scale, multi-model activities HTAP2, AQMEII3, and MICS-Asia3: Simulations, emission inventories, boundary conditions, and model output formats. *Atmos. Chem. Phys.* **17**, 1543-1555 (2017).
- S3. G. Janssens-Maenhout *et al.* HTAP_v2.2: A mosaic of regional and global emission grid maps for 2008 and 2010 to study hemispheric transport of air pollution. *Atmos. Chem. Phys.* **15**, 11411-11432 (2015).
- S4. J. N. Tan *et al.* Multi-model study of HTAP II on sulfur and nitrogen deposition. *Atmos. Chem. Phys.* **18**, 6847-6866 (2018).
- S5. J. Sun, J. S. Fu, J. A. Lynch, K. Huang, Y. Gao. Climate-driven exceedance of total (wet + dry) nitrogen (N) + sulfur (S) deposition to forest soil over the conterminous US. *Earths Future* **5**, 560-576 (2017).